

Technical Note: Towards Virtual Monitors for Image Guided Interventions Real-time Streaming to Optical See-Through Head-Mounted Displays

Long Qian, Mathias Unberath, Kevin Yu, Nassir Navab
Computer Aided Medical Procedures, Johns Hopkins University

Bernhard Fuerst
Computer Aided Medical Procedures, Johns Hopkins University
Bernhard Fuerst is now with Verb Surgical.

Alex Johnson, Greg Osgood
Department of Orthopaedic Surgery, Johns Hopkins University

(Dated: 4 February 2022)

Purpose: Image guidance is crucial for the success of many interventions. Images are displayed on designated monitors that cannot be positioned optimally due to sterility and spatial constraints. This indirect visualization causes potential occlusion, hinders hand-eye coordination, leads to increased procedure duration and surgeon load.

Methods: We propose a *virtual* monitor system that displays medical images in a mixed reality visualization using optical see-through head-mounted displays. The system streams high-resolution medical images from any modality to the head-mounted display in real-time that are blended with the surgical site. It allows for mixed reality visualization of images in head-, world-, or body-anchored mode and can thus be adapted to specific procedural needs.

Results: For typical image sizes, the proposed system exhibits an average end-to-end delay and refresh rate of 214 ± 30 ms and 41.4 ± 32.0 Hz, respectively.

Conclusions: The proposed *virtual* monitor system is capable of real-time mixed reality visualization of medical images. In future, we seek to conduct first pre-clinical studies to quantitatively assess the impact of the system on standard image guided procedures.

I. INTRODUCTION

Every day, countless image guided interventions are conducted by a diverse set of clinicians across many disciplines. From procedures performed by ultrasound technicians¹⁻³, to orthopaedic surgeons^{4,5}, to interventional radiologists^{6,7}, one aspect unites them all: the viewing of medical images on conventional monitors⁸⁻¹⁰. In many of the aforementioned interventional scenarios, real time images are acquired to guide the procedure. However, these images can only be viewed on designated wall mounted monitors. The ability to position these displays is limited due to sterility, flexibility as they are bound to mounts, and the spatial constraints of the room such as the operating team and equipment. Consequently, images designated for procedural guidance cannot be displayed in-line with the operative field^{8,9,11}. This indirect visualization with images visually off-axis from the intervention site has been shown to create a disconnect between the visuo-motor transformation hindering hand-eye coordination¹². Situations that allow for the viewing of ones hands and the guiding image simultaneously with an in-line view helps to solve this problem^{8,13-15}. To alleviate this problem, previous approaches placed miniature LCD displays close to the intervention site^{8,11} or displayed images via Google Glass^{15,16}. Unfortunately in all these cases, the small size and poor resolution of these displays limits the conveyable information impeding standalone use and, hence,

clinical relevance⁹.

Recent advances in optical see-through head-mounted display (OST-HMD) technology enable high resolution, binocular displays directly in the field of vision of the user without obstructing the rest of the visual scene^{17,18}. Coupled with medical imaging, this technology may provide *virtual* monitors that can be positioned close to the intervention site and are large enough to convey all required information. This technology has the potential to overcome aforementioned drawbacks. Our hypothesis is that the use of *virtual* displays based on OST-HMDs that enable in-line image guidance will allow clinicians to perform procedures with higher efficiency and with improved ergonomics over conventional monitors.

Within this technical note, we describe a setup for real-time streaming of high-resolution medical images to the Microsoft HoloLens¹⁹ that enables head-, world-, and body-anchored *virtual* monitors within the operating suite.

II. MATERIAL AND METHODS

II.A. System Overview

The concept of a virtual monitor for image-guided procedures can be realized via real-time streaming of the intra-procedurally acquired medical images or image sequences, i.e. video, to an optical see-through head-mounted display. The OST-HMD then visualizes the im-

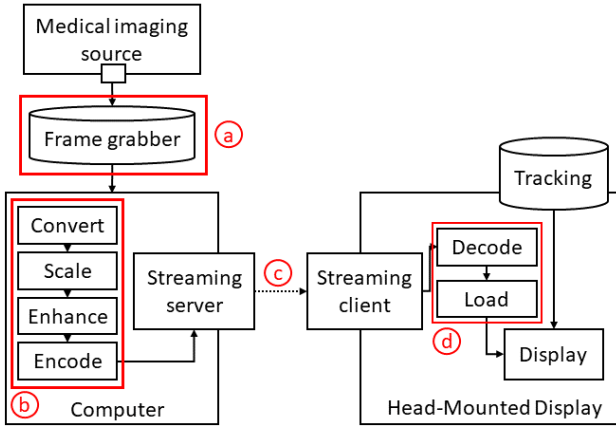


FIG. 1 Schematic overview of the system components and key functionality. Colored annotations highlight functionality modules that are potential bottlenecks for real-time streaming. Their individual performance is evaluated separately in section II.D.

ages, blending them with the reality perceived by the wearer. In the case presented here, we assume that the HMD is equipped with a tracking module. Then, medical images can be displayed in different modes allowing for different mixed reality experiences. A more detailed description of this circumstance is given in section II.C.2. Figure 1 demonstrates the components and functionalities of the proposed system. Components are introduced in section II.B while functionalities are described in detail in section II.C.

II.B. Material

II.B.1. Medical Imaging Source

Medical imaging sources provide input to the proposed real-time streaming pipeline. Potential medical imaging sources include 2D imaging modalities such as diagnostic X-ray fluoroscopy systems, interventional C-arm cone-beam scanners, and Ultrasound systems but naturally extends to 3D image sources including computed tomography, cone-beam computed tomography, and magnetic resonance imaging.

Traditionally, medical images are transferred within a vendor-specific framework inside the operating room. We use a video output port provided by the manufacturer to tap the medical imaging data after internal pre-processing that is simultaneously supplied to the traditional radiology monitors.

II.B.2. Frame Grabber

The frame grabber is hardware that is connected to a video output port of any imaging source (in this case a medical imaging modality) and has access to the imaging data. In setups where the medical imaging source provides an interface for direct access to the data, the frame grabber is not a necessary component. However, use of

a frame grabber has the additional benefit that it effectively decouples medical image generation and internal pre-preprocessing and the proposed streaming pipeline into two separate closed loops, such that the traditional imaging pipeline in the operating room remains unaffected.

II.B.3. Image Processing Framework

The image processing framework is responsible for converting, scaling, enhancing, and encoding the image at runtime. Memory-inefficient pixel formats can be converted to more efficient pixel format that allow for faster processing and transfer, e. g., a conversion from RGBA32 to YUV2, or to gray-scale. Scaling refers to the manipulation of the pixel size of the image and constitutes a trade-off between processing load and image quality. Enhancing is an optional step in the image processing pipeline. Well-known representatives of image processing filters are, e. g., contrast enhancement or denoising²⁰, that can be employed to further improve the perception and readability of the visualized medical images. Encoding describes the process of compressing images or fragmenting the data into smaller packets to enable efficient transfer or storage. Common encoders include, among others, Motion-JPEG²¹, H264²². Motion-JPEG is used in our setup.

II.B.4. Data Transfer Network

Data packets are transferred from the image processing framework to head-mounted display via a data transfer network. Depending on the specifications of the particular image processing framework and HMD device, the data transfer may happen locally, via cable, or via wireless router. For the setup described here we assume use of an untethered device. The image processing framework is realized on a stationary computer and, consequently, a wireless router (NETGEAR Nighthawk R6700²³) is used for communication and data transfer. TCP/IP²⁴ acts as the communication protocol.

II.B.5. Head-Mounted Display

The HMD receives the data packets from the data transfer network, decodes the data packets into images, and loads the decoded images into the rendering engine. Finally, it visualizes the sequence of images in a mixed reality environment with the help of tracking module. Within our experiments the Microsoft HoloLens^{19,25} is used as the mixed reality headset. An exemplary image of this OST-HMD that was released in March 2016²⁵ is provided in Figure 2.

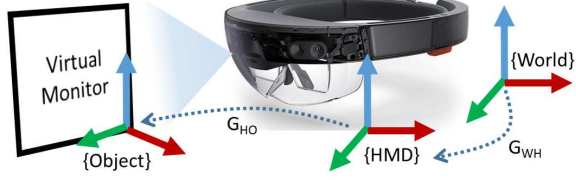


FIG. 2 Relevant transformations for visualization in mixed reality environments. The figure shows a Microsoft HoloLens, the image of which is taken from²⁹.

II.C. Methods

II.C.1. Tracking and Localization

Tracking and localization is the enabling mechanism for different mixed reality rendering effects. The virtual monitor effect requires the HMD to maintain knowledge about its position and orientation in the operating room, involving both hardware sensors and software algorithms. Common methods of tracking can be categorized into outside-in methods, such as external optical tracking²⁶, and inside-out approaches, e.g., simultaneous localization and mapping (SLAM)²⁷, that are employed in the scenario described here²⁵. The transformations between the coordinate systems of world, HMD and visualized object (here the *virtual* monitor) are demonstrated in Figure 2. Particularly, G_{WH} is the transformation from the world to the HMD coordinate system and is computed from the tracking module. G_{HO} describes the mapping from the HMD to the virtual object coordinate that is rendered on the HMD; it is controlled by the rendering algorithm. With Microsoft HoloLens, G_{WH} is computed from SLAM algorithms²⁸ and is available in real-time.

In the preceding description we have omitted that aforementioned transformations may not be constant over time. In fact, tracking of the relative movement of these coordinate systems is a key asset of the proposed pipeline, the reason of which is detailed below.

II.C.2. Mixed Reality Visualization

Aided by tracking and localization methods, the user is free to choose between three kinds of mixed reality visualization modes that are presented in the following sections. This flexibility in mixed reality experience is one of the major advancement of the proposed compared to earlier systems^{15,30}.

II.C.2.a. Head-Anchored In the head-anchored visualization, the rendered object is placed at a fixed pose relative to the user. This means that G_{HO} remains constant. In consequence, medical images are visualized in a head-up display manner. Researchers have exploited the benefits of head-anchored visualization in^{15,30,31}. Head-anchored visualization is powerful as it makes full use of the HMD in terms of visualization of the content. How-

ever, for cases where the surgeon does not want the medical images occluding potentially crucial areas of the operating field, head-anchored visualization is a distraction.

II.C.2.b. World-Anchored The world-anchored visualization is closest to current clinical practice. It creates a *virtual* monitor effect, where the user is able to see a medical imaging display as if it was presented on a traditional monitor. The 6 degree-of-freedom pose of the virtual object is invariant in the world coordinate system, i.e.,

$$G_{WO}(t) = G_{HO}(t) \cdot G_{WH}(t) = \text{const.}$$

$$G_{HO}(t) = G_{WO}(t) \cdot G_{WH}(t)^{-1}, \quad (1)$$

where t denotes the current time point as motivated in section II.C.1.

The rendering framework needs to incorporate real-time tracking results, and adjusts the pose of the virtual object accordingly. World-anchored visualization within the medical context has been studied in^{32,33}. World-anchored visualization is intuitive as it resembles the traditional monitor, and gives more control to the user in terms of the display configuration, e.g., with respect to location, orientation, and brightness.

II.C.2.c. Body-Anchored Body-anchored display is a concept that blends both head-anchored and world-anchored display. When the extent of the user's motion is large, the rendered virtual object follows the user's motion similar to head-anchored visualization. While the virtual object remains in the field-of-view of the user at all times, it is not necessarily always at the same pose as it would be in a head-anchored display. On the other hand, when the motion is small, which often happens when the user is slightly adjusting the viewing perspective to better perceive the virtual object, the virtual object remains fixed in the world space as a world-anchored display.

II.D. Experimental Validation

We quantitatively assess the performance of the key components of the proposed pipeline individually which then enables the computation of the total end-to-end performance. All components evaluated in this manner are highlighted by red boxes in Figure 1. This procedure allows for the identification of potential bottlenecks for system performance. All described measurements were repeated sufficiently many times (> 30) to ensure a representative set of samples.

II.D.1. Frame Grabber

We retrieve the delay of the frame grabber (component (a) in Figure 1) via a virtual stopwatch with a resolution of 15 ms and display the current time on the screen. The screen is then captured by the frame grabber, streamed to the same computer, and visualized in split screen. This technique allows for the computation of delay as we simultaneously display the current system and the captured video frame time.

The refresh rate of the frame grabber depends on the screen's resolution and computation power of the receiving computer. In our tests, we used an Epiphan DVI2USB 3.0 and an Alienware 15 R3 Laptop with Intel(R) Core i7-7700HQ equipped with a NVIDIA GeForce GTX 1070 operated at 1920×1080 pixels.

II.D.2. Image Processing

For the image processing pipeline, denoted by (b) in Figure 1, we assess the time between the moment the frame is available to the point when the frame is ready to be sent via the data transfer network. In our experiment, we use an incoming frame size of 1920×1080 pixels in RGB24 that is then down-sampled (scaled) to 800×450 pixels still in RGB24 format.

II.D.3. Data Transfer Network

Under normal circumstances, latency refers to the time that elapses between sending the frame from the host to receiving the same frame on the device, i.e. the HoloLens. Measuring latency in this setup, however, is complicated due to imperfect synchronization of host and device. In order to avoid inaccuracies due to synchronization, we rely on the HoloLens Emulator³⁴. Both, emulator and server, are running on the same machine thus sharing system time. In Figure 1, this delay is indicated as (c).

II.D.4. Head-Mounted Display

We measure the time on the device between receiving an image and loading the frame into the texture that is used for visualization, a delay that is denoted by (d) in the system overview shown in Figure 1. Moreover, We assess the rate of frame reception on the device and evaluate the texture loading time and the rendering refresh rate for multiple image sizes.

A more thorough evaluation of the display and tracking capabilities of a candidate OST-HMD is meaningful and important, particularly when considering applications in the medical context. This evaluation, however, is beyond the scope of the presented technical note. We would like to refer to a previous in-house study that compares multiple devices with respect to aforementioned criteria³⁵.

III. RESULTS

We state the average delay μ and the respective standard deviation σ for every of the aforementioned measurements in Table I. In summary, we found an average end-to-end transmission time of 214 ms (30 ms). The grabbing refresh rate was found to be a constant 36 Hz. Further, the number of received frames depending on the image size is stated in Table II. Finally, results for the texture loading time and refresh rate as a function of input image size are provided in Table III. Very high

TABLE I Average delay μ and standard deviation σ for the key components of the proposed network stated as μ (σ). All values are stated in ms.

(a) Grabbing	(b) Processing	(c) Transfer	(d) HMD
106 (29)	100 (7)	6.03 (2.28)	2.12 (3.71)

TABLE II Average number μ and standard deviation σ of received frames on the HMD device. All values stated in Hz.

620×480	800×450	1000×1000	1600×900	1920×1080
62.2 (44.6)	41.4 (32.0)	31.8 (23.7)	27.6 (19.4)	31.7 (26.2)

refresh rates above 30 Hz are achieved for image sizes smaller 1000×1000 pixels in RGB24.

IV. DISCUSSION

From our system evaluation presented in section II.D and section III, we computed an average end-to-end delay of 214 ms (30 ms) that may be sufficient for procedures that do not require very fast tool motion.

We have observed very high effective end-to-end frame rates of above 30 Hz for image sizes larger than 1000×1000 pixels in RGB24. Our findings suggest that, despite the large standard deviation of frame reception rate stated in Table II, the effective frame rate of the proposed *virtual* monitor system is limited by the texture rendering of the device.

Effective frame rates of 30 Hz with an average delay of 214 ms may not yet be convincing for optical video guided interventions using, e.g., endoscopy. However, we believe that the proposed system is fit for deployment in first pre-clinical studies in X-ray guided procedures. X-ray fluoroscopy is usually operated on lower frame rates (7.5 Hz to 30 Hz) to reduce exposure for both the patient and the surgeon³⁶.

From the detailed analysis shown in Table I we identified frame grabbing and image processing as the major bottlenecks with respect to delay, taking on average more than 100 ms each. The frame grabber comes with its proprietary driver and software and does not easily allow tweaks for performance. The image processing pipeline, however, potentially allows for modifications in future work that could target more efficient scaling and compression of the images.

The high standard deviation of the frame reception on the HMD device suggests bunching of incoming images. This behavior is not desirable, as it implies a varying

TABLE III Overall rendering refresh rate in Hz as a function of input image size. Images are RGB24.

Image size	(d) HMD μ (σ) in ms	Rendering μ (σ) in Hz
620×480	3.33 (8.83)	46.4 (6.7)
800×450	3.92 (10.47)	47.1 (6.5)
1000×1000	16.9 (34.2)	32.1 (9.2)
1600×900	25.7 (49.3)	22.5 (9.0)
1920×1080	61.3 (81.7)	16.4 (6.5)

frame rate and, thus, credibility of the displayed images at different time points during an image guided intervention. Future work will hence investigate possibilities of homogenizing the data transfer over time.

V. CONCLUSION

We have presented and evaluated an system for real-time visualization of medical images in a mixed reality surgical environment using an optical see-through head-mounted display. The system comprises of a frame grabber, an image processing unit, a data transfer network, and a head-mounted display. It accepts images of any conventional medical imaging modality. The current setup allows for real-time mixed reality visualization of medical images in head-, world-, and body-anchored display with an average delay of 214 ± 30 ms and a refresh rate of around 41.4 ± 32.0 Hz for typical image sizes. Given the promising results, we are excited to assess the impact of the system on the surgical work flow that we seek to study in first pre-clinical tests. Future improvements to the system will investigate means of stabilizing the refresh rate of the *virtual* monitor.

CONFLICTS OF INTEREST

The authors have no relevant conflicts of interest to disclose.

- ¹M Bajura, H Fuchs, and R Ohbuchi, "Merging virtual objects with the real world: Seeing ultrasound imagery within the patient," in *ACM SIGGRAPH Computer Graphics*, Vol. 26 (ACM, 1992) pp. 203–210.
- ²C M Rumack, S R Wilson, and J W Charboneau, *Diagnostic ultrasound vol 1* (London: Mosby, 2005, 2005).
- ³M Peterson and Z Basrai, "Introduction to Bedside Ultrasound," *Clinical Emergency Radiology*, 195 (2017).
- ⁴F F Strobl, S M Haeussler, P M Paprottka, *et al.*, "Technical and clinical outcome of percutaneous CT fluoroscopy-guided screw placement in unstable injuries of the posterior pelvic ring," *Skeletal Radiology* **43**, 1093–1100 (2014).
- ⁵T De Silva, J Punnoose, A Uneri, *et al.*, "C-arm positioning using virtual fluoroscopy for image-guided surgery," in *SPIE Medical Imaging* (International Society for Optics and Photonics, 2017) pp. 101352K–101352K.
- ⁶V Tacher, M Lin, P Desgranges, *et al.*, "Image guidance for endovascular repair of complex aortic aneurysms: comparison of two-dimensional and three-dimensional angiography and image fusion," *Journal of Vascular and Interventional Radiology* **24**, 1698–1706 (2013).
- ⁷A Mason, R Paulsen, J M Babuska, *et al.*, "The accuracy of pedicle screw placement using intraoperative image guidance systems: A systematic review," *Journal of Neurosurgery: Spine* **20**, 196–203 (2014).
- ⁸J D Westwood, "The mini-screen: an innovative device for computer assisted surgery systems," *Medicine Meets Virtual Reality 13: The Magical Next Becomes the Medical Now* **111**, 314 (2005).
- ⁹Z Yaniv and K Cleary, "Image-guided procedures: A review," *Computer Aided Interventions and Medical Robotics* **3**, 1–63 (2006).
- ¹⁰R J Hallifax, J P Corcoran, A Ahmed, *et al.*, "Physician-based ultrasound-guided biopsy for diagnosing pleural disease," *Chest* **146**, 1001–1006 (2014).
- ¹¹M A Cardin, J X Wang, and D B Plewes, "A method to evaluate human spatial coordination interfaces for computer-assisted surgery," *Medical Image Computing and Computer-Assisted Intervention–MICCAI 2005*, 9–16 (2005).
- ¹²B Wentink, "Eye-hand coordination in laparoscopy – an overview of experiments and supporting aids," *Minimally Invasive Therapy & Allied Technologies* **10**, 155–162 (2001).
- ¹³G B Hanna, S M Shimi, and A Cuschieri, "Task performance in endoscopic surgery is influenced by location of the image display," *Annals of surgery* **227**, 481 (1998).
- ¹⁴K Erfanian, F I Luks, A G Kurkchubasche, C W Wesselhoeft, and T F Tracy, "In-line image projection accelerates task performance in laparoscopic appendectomy," *Journal of pediatric surgery* **38**, 1059–1062 (2003).
- ¹⁵P C Chimenti and D J Mitten, "Google Glass as an alternative to standard fluoroscopic visualization for percutaneous fixation of hand fractures: a pilot study," *Plastic and Reconstructive Surgery* **136**, 328–330 (2015).
- ¹⁶J W Yoon, R E Chen, P K Han, P Si, W D Freeman, and S M Pirris, "Technical feasibility and safety of an intraoperative head-up display device during spine instrumentation," *The International Journal of Medical Robotics and Computer Assisted Surgery* (2016).
- ¹⁷K Keller, A State, and H Fuchs, "Head mounted displays for medical use," *Journal of Display Technology* **4**, 468–472 (2008).
- ¹⁸M H Iqbal, A Aydin, O Bruckhorst, P Dasgupta, and K Ahmed, "A review of wearable technology in medicine," *Journal of the Royal Society of Medicine* **109**, 372–380 (2016).
- ¹⁹"Microsoft HoloLens," <https://www.microsoft.com/en-us/hololens> (2017), accessed: 2017-06-21.
- ²⁰M Sonka, V Hlavac, and R Boyle, *Image processing, analysis, and machine vision* (Cengage Learning, 2014).
- ²¹J Mohr, "Motion jpeg 2000 and iso base media file format (parts 3 and 12)," in *The JPEG 2000 Suite* (John Wiley & Sons, Ltd, 2009) pp. 109–119.
- ²²D Marpe, T Wiegand, and G J Sullivan, "The H. 264/MPEG4 advanced video coding standard and its applications," *IEEE Communications Magazine* **44**, 134–143 (2006).
- ²³"NETGEAR Nighthawk R6700," <https://www.netgear.com/home/products/networking/wifi-routers/R6700>. (2017), Accessed: 2017-06-21.
- ²⁴L Parziale, W Liu, C Matthews, *et al.*, *TCP/IP tutorial and technical overview* (IBM Redbooks, 2006).
- ²⁵B C Kress and W J Cummings, "11-1: Invited paper: Towards the ultimate mixed reality experience: HoloLens display architecture choices," *SID Symposium Digest of Technical Papers* **48**, 127–131 (2017).
- ²⁶R Khadem, C C Yeh, M Sadeghi-Tehrani, *et al.*, "Comparative tracking error analysis of five different optical tracking systems," *Computer Aided Surgery* **5**, 98–107 (2000).
- ²⁷H Durrant-Whyte and T Bailey, "Simultaneous localization and mapping: part i," *IEEE robotics & automation magazine* **13**, 99–110 (2006).
- ²⁸L Qian, E Azimi, P Kazanzides, and N Navab, "Comprehensive Tracker Based Display Calibration for Holographic Optical See-Through Head-Mounted Display," *arXiv* (2017).
- ²⁹"Microsoft Press Tools: HoloLens," https://news.microsoft.com/mshololens_hero1_rgb/#h6jwDUHewTJrbBM6.97 (2017), accessed: 2017-06-21.
- ³⁰B Hannaford, J K Barral, E Rephaeli, C D Ching, and V S Bajaj, "Heads-up displays for augmented reality network in a medical environment," (2017), uS Patent 9,645,785.
- ³¹W Vorraber, S Voessner, G Stark, D Neubacher, S DeMello, and A Bair, "Medical applications of near-eye display devices: an exploratory study," *International Journal of Surgery* **12**, 1266–1272 (2014).
- ³²X Chen, L Xu, Y Wang, *et al.*, "Development of a surgical navigation system based on augmented reality using an optical see-through head-mounted display," *Journal of Biomedical Informatics* **55**, 124–131 (2015).
- ³³H Wang, F Wang, A P Y Leong, L Xu, X Chen, and Q Wang, "Precision insertion of percutaneous sacroiliac screws using a novel augmented reality-based navigation system: a pilot study," *International Orthopaedics* **40**, 1941–1947 (2016).

- ³⁴ “Microsoft HoloLens Emulator,” <https://developer.microsoft.com/en-us/windows/mixed-reality/using-the-holo-lens-emulator> (2017), accessed: 2017-06-21.
- ³⁵ L Qian, A Barthel, A Johnson, *et al.*, “Comparison of optical see-through head-mounted displays for surgical interventions with object-anchored 2D-display,” International Journal of Computer Assisted Radiology and Surgery , 1–10 (2017).
- ³⁶ M Mahesh, “Fluoroscopy: patient radiation exposure issues 1,” Radiographics **21**, 1033–1045 (2001).